Cross-Channel Impedance Measurement for Monitoring Implanted Electrodes

(article starts on next page)

Cross-Channel Impedance Measurement for Monitoring Implanted Electrodes

Eric J. Earley, *Member, IEEE*, Enzo Mastinu, *Member, IEEE*, and Max Ortiz-Catalan, *Senior Member, IEEE*

Abstract— Implanted electrodes, such as those used for cochlear implants, brain-computer interfaces, and prosthetic limbs, rely on particular electrical conditions for optimal operation. Measurements of electrical impedance can be a diagnostic tool to monitor implanted electrodes for changing conditions arising from glial scarring, encapsulation, and shorted or broken wires. Such measurements provide information about the electrical impedance between a single electrode and its electrical reference, but offer no insights into the overall network of impedances between electrodes. Other solutions generally rely on geometrical assumptions of the arrangement of the electrodes and may not generalize to other electrode networks. Here, we propose a linear algebra-based approach, Cross-Channel Impedance Measurement (CCIM), for measuring a network of impedances between electrodes which all share a common electrical reference. This is accomplished by measuring the voltage response from all electrodes to a known current applied between each electrode and the shared reference, and is agnostic to the number and arrangement of electrodes. The approach is validated using a simulated 8-electrode network, demonstrating direct impedance measurements between electrodes and the reference with 96.6% ± 0.2% accuracy, and cross-channel impedance measurements with 93.3% ± 0.6% accuracy in a typical system. Subsequent analyses on randomized systems demonstrate the sensitivity of the model to impedance range and measurement noise.

Clinical Relevance—CCIM provides a system-agnostic diagnostic test for implanted electrode networks, which may aid in the longitudinal tracking of electrode performance and early identification of electronics failures.

I. INTRODUCTION

Medical devices are becoming more reliant on the acquisition of biosignals (EMG, EKG, EEG), especially for monitoring and controlling robotic devices. However, as greater selectivity becomes a more frequent need for these medical devices, researchers are turning to implantable sensors to acquire these signals. Implantable sensors, such as the epimysial, intramuscular, and cuff electrodes often used in prosthetic limb control [1], [2] and the microelectrode arrays used with neural tissues [3]–[5], are typically made of biologically inert materials such as platinum, titanium, or tungsten to maximize biocompatibility and reduce risk of adverse immune response [6]. However, biological responses and microglial processes can impair the performance of these electrodes over time. Thus, the monitoring of these electrodes is imperative for researchers in these fields [7].

The connectivity of electrodes is commonly monitored by measuring the electrical impedance between electrodes and the reference. This is commonly done by sending electrical current with a known amplitude between each electrode and its reference, and measuring the resulting voltage [8]. Although this simple method can provide information about the general connectivity for each electrode, it fails to provide detailed information about the network of impedances between electrodes, and therefore cannot diagnose issues such as shorted electrodes. Other approaches rely on more complex modeling of the impedance within a system. However, methods such as four-point impedance [9] and four-electrode reflection-coefficient techniques [10], often used in cochlear implants, or electrochemical impedance spectroscopy [11], [12] rely on prior knowledge of the geometry or arrangement of the electrodes.

In this manuscript, we propose an approach to measure a network of impedances between implanted electrodes which all share a common electrical reference. This approach, which we term Cross-Channel Impedance Measurement (CCIM) relies on a linear series of equations which can be solved directly using linear algebra. Validation of the approach using simulations yielded accuracy greater than 93% under typical conditions. Moreover, a subsequent analysis with random networks demonstrated the sensitivity of the approach to measurement noise and the range of network impedances to be measured, ultimately providing guidelines and limitations for the use of CCIM in other applications.

II. METHODS

A. General Impedance Measurement

Consider an implanted system comprising N electrodes, each sharing a common electrical reference. A straightforward method of measuring the electrical impedance Z_i between an electrode and the reference is to send a current of known amplitude I_{in} between the electrode and the reference, and measure the amplitude of the resulting voltage V_i. Then, the impedance is calculated as per Ohm's Law:

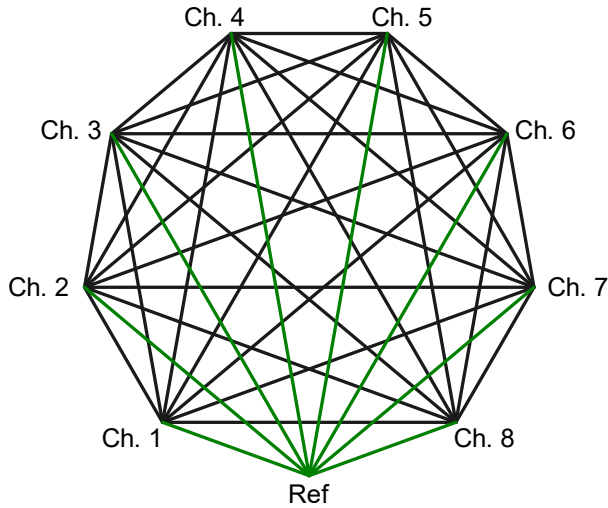$$|Z_i| = \frac{|V_i|}{|I_{in}|} \qquad (1)$$

Fig. 1 An example electrode system visually represented as a complete graph K_9, comprising 8 electrodes and 1 shared reference. This system can be considered as a set of 36 impedances, defined as 8 direct impedances (green, between each electrode and the shared reference) and 28 cross-channel impedances (black, between pairs of electrodes). During CCIM, current is passed between one electrode and the reference, and the resulting voltage is measured between each electrode and the reference.

We note that biological tissue is known to elicit both resistive and capacitive response to electrical current; thus, for the purposes of this manuscript, we consider $|I_{in}|$ and $|V_i|$ to be the steady-state amplitude of a sinusoidal current input and voltage output, respectively, and we therefore consider $|Z_i|$ to be the total impedance magnitude combining resistive and capacitive responses.

This method of impedance measurement is simple and effective at monitoring general electrical characteristics of the implanted system, and can be used to identify common issues such as disconnected electrodes. However, this implementation does not explicitly consider that electrodes may not be completely insulated from one another. For example, if an electrical short exists between two electrodes, a general impedance measurement would only show that the two electrodes have nearly identical impedance, but cannot reveal the underlying mechanism. Instead, an impedance measurement model must consider the interconnectivity between all electrodes in the system.

B. Cross-Channel Impedance Measurement

For the purposes of this manuscript, we assume a rather pessimistic but nevertheless realistic scenario where no electrodes are completely insulated from one another and therefore all are electrically connected. Thus, some portion of the current entering the system through one electrode passes by the tissues measured by each other electrode (hereinafter referred to as "nodes") on its path to the reference. This system can be represented visually as a complete graph K_{N+1}, where $N + 1$ comprises N electrodes and 1 electrical reference (8-electrode example in **Fig. 1**). For this system, the total number of current paths, and therefore the total number of impedances, is calculated as:

$$N_Z = \frac{N(N+1)}{2} \qquad (2)$$

These impedances are distinguished between direct impedance (the impedance between an electrode and the reference) and cross-channel impedance (the impedance between two nodes).

While sending current through electrode i, the current flowing in and out of node j is described according to Kirchoff's Current Law:

$$|I_{j,i}| = \frac{|V_{j,i}|}{|Z_{j,j}|} + \sum_{k \neq j}^{N} \frac{(|V_{j,i}| - |V_{k,i}|)}{|Z_{j,k}|} \qquad (3)$$

where $|V_{j,i}|$ is the voltage measured between electrode j and the reference during stimulation of electrode i, $|Z_{j,j}|$ is the direct impedance between node j and the reference, $|Z_{j,k}|$ is the cross-channel impedance between nodes j and k, and:

$$|I_{j,i}| = \begin{cases} I_{in}, i = j \\ 0, i \neq j \end{cases} \qquad (4)$$

Equation (3) can be further simplified by replacing impedance with admittance:

$$|Y| = \frac{1}{|Z|} \qquad (5)$$

Applying (5) to (3) yields:

$$|I_{j,i}| = |V_{j,i}||Y_{j,j}| + \sum_{k \neq j}^{N}(|V_{j,i}| - |V_{k,i}|)|Y_{j,k}| \qquad (6)$$

As a symmetric and strongly regular graph, (6) is generalizable to any combination of stimulating and recording electrodes. Thus, Equations (4) and (6) generates a system of N_Z linear equations which can be arranged as follows:

$$I = UY \qquad (7)$$

Equation (7) can be solved by populating sparse matrices I and U according to Algorithm 1, and the resulting admittance matrix takes the form:

$$Y = [|Y_{1,1}|...|Y_{1,N}||Y_{2,2}|...|Y_{2,N}||Y_{3,3}|...|Y_{N,N}|]^T \qquad (8)$$

Calculating the reciprocal of each element of Y yields all impedances within the system.

C. Model Validation

Two sets of tests were conducted to validate and characterize CCIM performance. First, a simulation of an 8-electrode system tested the accuracy and precision of CCIM for three test cases representing ideal and unideal conditions, as well as the general performance of CCIM during random conditions. The simulation also allowed for characterization of the performance degradation due to increasing measurement noise. Second, a physical model of a 4-electrode system was built on a breadboard to test the robustness of CCIM to human voltage measurement.

All materials used to validate CCIM are available on the Open Science Framework [13].

1) Defined 8-Electrode Simulated Measurements

An 8-electrode system was simulated in Simulink (MATLAB 2021b, MathWorks) to characterize the performance of CCIM in three examples: an ideal system with
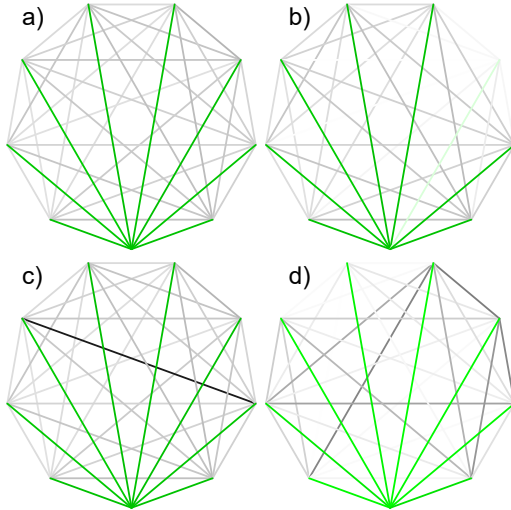
Fig. 2 With a simulated 8-electrode system, CCIM performance was characterized for (a) an ideal system with low low direct impedance (dark green) and higher cross-channel impedance (grey), (b) a system with electrode 6 disconnected as signified by high impedances (light green and light grey), (c) a system with a short between electrodes 3 and 7 (black), and (d) systems with randomly selected impedances. Lighter colors indicate high impedance, darker colors indicate low impedance.

Algorithm 1 Calculating Admittances Y for complete graph K_{N+1}
Input: Number of electrodes N, input current $\|I_{in}\|$, voltage measurements $\|V_{j,i}\|$ where $\|V_{j,i}\| = \|V_{i,j}\|$
Output: N_Z x 1 admittance matrix Y

1. $I \leftarrow N_Z$ x 1 sparse matrix
2. $U \leftarrow N_Z$ x N_Z sparse matrix
3. $c \leftarrow 0$
4.   **for** $i \leftarrow$ stimulation electrodes 1 to N **do**
5.   **for** $j \leftarrow$ measurement electrodes i to N **do**
6. $c \leftarrow c + 1$
7.   **if** $i = j$
8. $I_{c,1} \leftarrow \|I_{in}\|$
9.   **end if**
10.   **for** $k \leftarrow$ electrodes 1 to N **do**
11. $a \leftarrow max\,(j, k)$
12. $b \leftarrow min\,(j, k)$
13. $d \leftarrow a + (b - 1)(N - b/2)$
14.   **if** $j = k$ **then**
15. $U_{c,d} \leftarrow \|V_{j,i}\|$
16.   **else then**
17. $U_{c,d} \leftarrow \|V_{j,i}\| - \|V_{k,i}\|$
18.   **end if**
19.   **end for**
20.   **end for**
21.   **end for**
22. $Y \leftarrow U \backslash I$
23.   **return** Y

low direct impedance and higher cross-channel impedance (**Fig. 2a**), a system with one disconnected electrode (**Fig. 2b**), and a system with a short between electrodes 3 and 7 (**Fig. 2c**).

2) Randomized 8-Electrode Simulated Measurements

A second analysis simulated a range of system impedances and levels of measurement noise to determine the generalizability of CCIM (**Fig. 2d**). The minimum and maximum impedance within the system ranged from 1 Ω to 1 MΩ, and the level of measurement noise ranged from 0% to 5%; for each condition, errors were averaged across 10 iterations. A linear model estimated the impact of the impedance magnitude and type, system impedance range, and magnitude of measurement noise on the overall measurement error.

3) 4-Electrode Physical Measurements

A 4-electrode system was assembled on a prototyping board to validate CCIM using voltage measured directly by an experimenter. System impedances ranged from 1.5 kΩ to 470 kΩ, and the voltage between each electrode and the reference arising from a 1 mA DC current was measured using an oscilloscope.

III. Results

The validation of CCIM describes the precision of the calculations with respect to different impedance magnitudes and measurement error. This can be used to determine the viability of CCIM for different research areas, implantable electrode systems, and measurement devices.

A. 8-Electrode Simulated Measurements

CCIM calculated the impedances within the ideal system with median errors of less than 0.1% when estimating direct impedances, and 3.5% ± 1.4% (median ± IQR) when estimating cross-channel impedances. When measurement noise increased to 5%, impedance calculation errors also increased to 3.4% ± 0.2% (median ± IQR) for direct impedances, and 6.7% ± 0.6% for cross-channel impedances.

For the purposes of comparison, results for **Fig. 2b-c** are presented assuming 5% measurement noise. When simulating a disconnected electrode (**Fig. 2b**), unaffected impedances were calculated with similar precision to the ideal system. However, impedance estimates of the disconnected electrode were substantially higher: 43.9% error estimating the direct impedance, and 9.2% ± 6.7% estimating the cross-channel impedances. CCIM performed similarly when estimating direct impedances in a system with two shorted electrodes (**Fig. 2c**), although errors were substantially higher for the direct impedances of the affected electrodes (51.8% ± 1.8%). Cross-channel impedance calculation error was also higher for those impedances connected to the affected node (83.6% ± 43%) than for those that are not (7.5 ± 36.3%).

The magnitude of impedance calculation errors, as affected by the measured impedance, range of system impedances, and measurement error, is shown in **Fig. 3**. Statistical analysis using a linear model revealed significant interactions between factors, meaning that the impact of each factor cannot easily be generalized. However, several trends do appear consistent across conditions.

Generally, higher impedances were estimated with higher error using CCIM. More notably, however, is that the introduction of voltage measurement noise significantly increases the errors in impedance calculations. For example, at lower impedances, errors were well below 1% with no voltage measurement noise, but increased upwards of 1% with a low measurement noise of 1%.

An interesting behavior occurs when a system comprises a larger range of impedances. When impedance values are more similar (**Fig. 3**, dark lines) the average error tends to remain consistent regardless of the magnitude of those impedances.
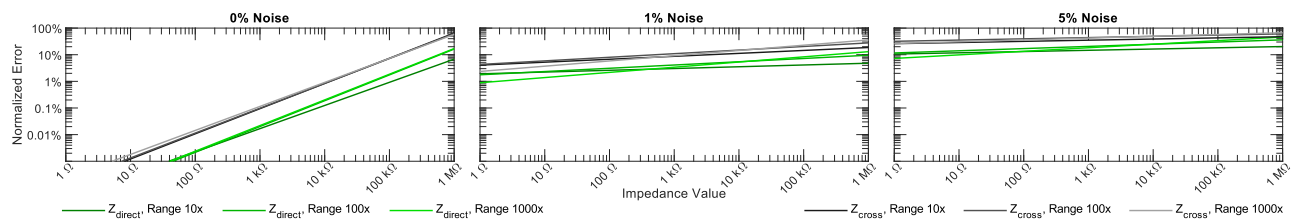
Fig. 3 Validation of CCIM demonstrates the theoretical performance across a range of impedance values with no measurement error, as well as the effect of increasing measurement error on this performance. Expected errors when calculating direct impedances are lower than cross-channel impedances, and the range of errors widens with a widening range of impedance values within the system.

However, when impedance values vary from one another by up to a factor of a thousand (**Fig. 3**, light lines), CCIM error also vary more widely, with lower errors for small impedances and higher errors for larger impedances.

B. 4-Electrode Physical Measurements

Calculating impedances using manually acquired voltage measurements demonstrated the general reliability of CCIM. Average errors for direct impedances were $5.5\% \pm 6.3\%$, for cross-channel impedances were $6.7\% \pm 4.3\%$.

IV. Discussion

The purpose of this study is to propose a method of estimating a network of impedances within a system of implanted electrodes sharing a common reference. Validation with the defined systems (**Fig. 2a-c**) demonstrated impedance estimate errors of 3.4% and 6.7% for direct and cross-channel impedances, respectively. CCIM is agnostic to the number and arrangement of the electrodes, making it potentially applicable to a wide range of implantable systems.

A. Limitations

As shown in **Fig. 3**, the precision of the impedance calculation is highly dependent on the noise of the voltage measurements. At 1% noise, direct impedance measurements are made with 1% to 10% error, but increasing the noise to 5% subsequently increased errors to between 10% and 40%. This suggests that accurate voltage measurements are increasingly important for higher-impedance systems.

Errors tended to increase for impedances connected to a shorted or disconnected electrodes; this was mirrored with the randomized simulations, where errors tended to increase with a wider range of impedance magnitudes within the system.

B. Future Developments

One area of possible future improvement is to conduct iterative checks on the calculated impedances from CCIM to remove functionally irrelevant impedances from the system. For example, **Fig. 2b** depicts a system where one electrode is disconnected from the rest of the system. If this is the case, one may be able to remove the electrode and all its connections from the analysis, simplifying the model. Alternatively, **Fig. 2c** depicts a system where two electrodes are shorted. In such a situation, one may be able to merge the two electrodes into a single node, again simplifying the model. Both approaches, if iterated, could be used to improve CCIM performance by reducing the number of terms in the system of equations, and by merging parallel impedances into a single equivalent impedance in cases with a short, thus allowing CCIM to identify electrical issues while still characterizing the working components of the implanted system.

V. References

[1] M. Ortiz-Catalan, B. Håkansson, and R. Brånemark, "An osseointegrated human-machine gateway for long-term sensory feedback and motor control of artificial limbs," *Sci. Transl. Med.*, vol. 6, no. 257, 2014, doi: 10.1126/scitranslmed.3008933.

[2] M. Ortiz-Catalan, E. Mastinu, P. Sassu, O. Aszmann, and R. Brånemark, "Self-Contained Neuromusculoskeletal Arm Prostheses," *N. Engl. J. Med.*, vol. 382, no. 18, pp. 1732–1738, Apr. 2020, doi: 10.1056/NEJMoa1917537.

[3] E. M. Maynard, C. T. Nordhausen, and R. A. Normann, "The Utah Intracortical Electrode Array: A recording structure for potential brain-computer interfaces," *Electroencephalogr. Clin. Neurophysiol.*, vol. 102, no. 3, pp. 228–239, 1997, doi: 10.1016/S0013-4694(96)95176-0.

[4] S. Bredeson, A. Kanneganti, F. Deku, S. Cogan, M. Romero-Ortega, and P. Troyk, "Chronic in-vivo testing of a 16-channel implantable wireless neural stimulator," *Proc. Annu. Int. Conf. IEEE Eng. Med. Biol. Soc. EMBS*, vol. 2015-Novem, pp. 1017–1020, 2015, doi: 10.1109/EMBC.2015.7318537.

[5] N. M. Dotson, S. J. Hoffman, B. Goodell, and C. M. Gray, "A Large-Scale Semi-Chronic Microdrive Recording System for Non-Human Primates," *Neuron*, vol. 96, no. 4, pp. 769-782.e2, 2017, doi: 10.1016/j.neuron.2017.09.050.

[6] D. F. Williams, "On the mechanisms of biocompatibility," *Biomaterials*, vol. 29, no. 20, pp. 2941–2953, 2008, doi: 10.1016/j.biomaterials.2008.04.023.

[7] P. A. Cody, J. R. Eles, C. F. Lagenaur, T. D. Y. Kozai, and X. T. Cui, "Unique electrophysiological and impedance signatures between encapsulation types: An analysis of biological Utah array failure and benefit of a biomimetic coating in a rat model," *Biomaterials*, vol. 161, pp. 117–128, 2018, doi: 10.1016/j.biomaterials.2018.01.025.

[8] Z. Hu, P. Troyk, G. Demichele, D. Kerns, and M. Bak, "A laboratory instrument for characterizing multiple microelectrodes," *Proc. Annu. Int. Conf. IEEE Eng. Med. Biol. Soc. EMBS*, pp. 1558–1561, 2013, doi: 10.1109/EMBC.2013.6609811.

[9] C. Bester *et al.*, "Four-point impedance as a biomarker for bleeding during cochlear implantation," *Sci. Rep.*, vol. 10, no. 1, pp. 1–12, 2020, doi: 10.1038/s41598-019-56253-w.

[10] G. Kumar, M. Chokshi, and C. P. Richter, "Electrical impedance measurements of cochlear structures using the four-electrode reflection-coefficient technique," *Hear. Res.*, vol. 259, no. 1–2, pp. 86–94, 2010, doi: 10.1016/j.heares.2009.10.010.

[11] A. J. Bard and L. R. Faulkner, *Electrochemical Methods: Fundamentals and Applications*, 2nd ed. New York: Wiley, 2002.

[12] S. Wang, J. Zhang, O. Gharbi, V. Vivier, M. Gao, and M. E. Orazem, "Electrochemical impedance spectroscopy," *Nat. Rev. Methods Prim.*, vol. 1, no. 1, p. 41, Dec. 2021, doi: 10.1038/s43586-021-00039-w.

[13] E. J. Earley and M. Ortiz-Catalan, "Cross-Channel Impedance Measurement for Monitoring Implanted Electrodes," 2022. [Online]. Available: https://osf.io/3h7ny/.